https://doi.org/10.1093/plphys/kiab545 PLANT PHYSIOLOGY 2022: 188: 1483–1495

Plant Physiology®

Research Article

Reciprocal mutations of two multifunctional β-amyrin synthases from *Barbarea vulgaris* shift α/β-amyrin ratios

Jan Günther [1], Pernille Østerbye Erthmann [1], Bekzod Khakimov[1,2] and Søren Bak [1,*,†]

1 Department of Plant and Environmental Sciences and Copenhagen Plant Science Center, University of Copenhagen, Denmark
2 Department of Food Science, University of Copenhagen, Denmark

*Author for communication: bak@plen.ku.dk
These authors contributed equally (J.G., P.Ø.E.).
†Senior author.
The author responsible for distribution of materials integral to the findings presented in this article in accordance with the policy described in the Instructions for Authors (https://academic.oup.com/plphys/pages/general-instructions) is: Søren Bak (bak@plen.ku.dk).

Abstract

In the wild cruciferous wintercress (*Barbarea vulgaris*), β-amyrin-derived saponins are involved in resistance against insect herbivores like the major agricultural pest diamondback moth (*Plutella xylostella*). Enzymes belonging to the 2,3-oxidosqualene cyclase family have been identified and characterized in *B. vulgaris* G-type and P-type plants that differ in their natural habitat, insect resistance and saponin content. Both G-type and P-type plants possess highly similar 2,3-oxidosqualene cyclase enzymes that mainly produce β-amyrin (*Barbarea vulgaris* Lupeol synthase 5 G-Type; *Bv*LUP5-G) or α-amyrin (*Barbarea vulgaris* Lupeol synthase 5 P-Type; *Bv*LUP5-P), respectively. Despite the difference in product formation, the two *Bv*LUP5 enzymes are 98% identical at the amino acid level. This provides a unique opportunity to investigate determinants of product formation, using the *B. vulgaris* 2,3-oxidosqualene cyclase enzymes as a model for studying amino acid residues that determine differences in product formation. In this study, we identified two amino acid residues at position 121 and 735 that are responsible for the dominant changes in generated product ratios of β-amyrin and α-amyrin in both *Bv*LUP5 enzymes. These amino acid residues have not previously been highlighted as directly involved in 2,3-oxidosqualene cyclase product specificity. Our results highlight the functional diversity and promiscuity of 2,3-oxidosqualene cyclase enzymes. These enzymes serve as important mediators of metabolic plasticity throughout plant evolution.

Introduction

Triterpenoid saponins are specialized metabolites produced by diverse organisms, including plants and marine animals (Augustin et al., 2011; Thimmappa et al., 2014). Structurally, saponins represent a highly diverse subclass of terpenoids comprising more than 200 different triterpenoid backbone structures (Xu et al., 2004; Augustin et al., 2011). Saponins are amphipathic molecules composed of a hydrophobic triterpenoid portion, derived from a limited number of core backbone structures, and a hydrophilic glycosidic portion (Augustin et al., 2011). This combination of both hydrophobic and hydrophilic character provides saponins detergent-like properties (Chen et al., 2010; Lorent et al., 2014; Moses et al., 2014; Jiang et al., 2018). Saponins are structurally related to sterols and steroid hormones and therefore can interfere with sterols in cell membranes, which may lead to deleterious pore formation that causes cell death (Augustin et al., 2011). These properties have been proposed to

Received July 27, 2021. Accepted October 25, 2021. Advance access publication December 1, 2021

manifest their main insecticidal activities in plants (Kuzina et al., 2009; Khakimov et al., 2015; Liu et al., 2019).

Within the plant kingdom, saponins occur in several unrelated plant families acting as specialized metabolites involved in defense and disease resistance (Papadopoulou et al., 1999; Haralampidis et al., 2001; Shiu et al., 2004). In the extended Brassicaceae family only bittercress (*Babarea vulgaris*) is known to accumulate saponins, indicating that this is a rather recent evolutionary trait (Shinoda et al., 2002; Agerbirk et al., 2003; Nielsen et al., 2010a, 2010b; Badenes-Perez et al., 2014). In the *B. vulgaris* complex, there are distinctive plant types that have been shown to largely vary in their insect resistance, glucosinolate and saponin composition, trichome density, as well as geographic distribution (Christensen et al., 2014). Here, Pubescent (P-type) *B. vulgaris* plants that are rich in trichomes have a more present distribution in Eastern Europe and are susceptible to insect herbivores like the diamond back moth (*Plutella xylostella*; Agerbirk et al., 2003; Khakimov et al., 2015) and flea beetle larvae (*Phyllotreta nemorum*; Kuzina et al., 2009, 2011; Christensen et al., 2014). Instead, Glabrous (G-type) *B. vulgaris* plants with lower trichome density predominate in Western Europe and are highly deterrent to these herbivores (Hauser et al., 2012; Christensen et al., 2019). This insect deterrence in *B. vulgaris* G-type plants has been associated with the production of specific saponins (Kuzina et al., 2011; Khakimov et al., 2015; Byrne et al., 2017; Liu et al., 2019). Despite their genotypic similarity, G-type plants biosynthesize insecticidal saponins, whereas P-type plants lack this ability. Comparative quantitative trait loci (QTL) analysis of G-type and P-type *B. vulgaris* plants revealed that saponin-mediated insect resistance traits co-localize with two loci (*B. vulgaris* Lupeol synthase 5; *BvLUP5* and *B. vulgaris* Lupeol synthase 2; *BvLUP2*) that could be identified as 2,3-oxidosqualene cyclase genes (Byrne et al., 2017).

Generally, 2,3-oxidosqualene cyclases (OSCs) catalyze the first committed step of the biosynthesis of triterpenoid saponins by cyclization of 2,3-oxidosqualene (Phillips et al., 2006; Xue et al., 2012; Thimmappa et al., 2014; Cárdenas et al., 2019). In *B. vulgaris*, triterpenoid core structures are subsequently oxygenated by cytochrome P450 enzymes (Liu et al., 2019) and glucosylated by UDP-glucosyl transferase enzymes (Augustin et al., 2011; Khakimov et al., 2015; Erthmann et al., 2018) to produce saponins involved in resistance toward the agricultural pest diamondback moths (*Plutella xylostella*) and flea beetles *Phyllotreta nemorum* (Nielsen and Engelbrecht, 1997; Shinoda et al., 2002; Agerbirk et al., 2003; Kuzina et al., 2009). Both P- and G-type plants possess the *BvLUP5* and *BvLUP2* gene; however, their expression profile differs amongst these subspecies (Khakimov et al., 2015). The expression of *BvLUP5* is predominant in G-type plants, whereas *BvLUP2* expression is higher in P-type plants. Corresponding to these expression patterns, G-type plants predominantly produce β-amyrin-derived saponins, while P-type plants predominantly produce lupeol-derived saponins (Khakimov et al., 2015; Khakimov et al., 2016). We have previously shown that the β-amyrin-derived saponin hederagenin cellobioside confers resistance to insect pests in *B. vulgaris* G-type plants (Liu et al., 2019). Furthermore, transient expression of G-type and P-type *BvLUP5* in *Nicotiana benthamiana* mainly resulted in a differential accumulation of β-amyrin and α-amyrin, where the G-type enzyme produces a 6.5 ratio and the P-type *Bv*LUP5 a much lower ratio of 0.6 (Khakimov et al., 2015). Despite this 10-fold difference in product ratio, the two *Bv*LUP5 enzymes share an amino acid identity of 98%, corresponding to only 14 amino acid residues differences (Khakimov et al., 2015). The high sequence identity and the differences in product ratios make the *B. vulgaris* LUP5 OSCs an excellent model for studying amino acid residues that are responsible for the difference in OSC product formation. Furthermore, observed sequence alterations highlights amino acid residues that are evolutionarily important for facilitating crucial steps in β-amyrin-derived herbivore resistance in *B. vulgaris* (Byrne et al., 2017; Cárdenas et al., 2019). In recent years, the identification and characterization of numerous divergent OSCs from plants has facilitated the accurate differentiation of OSCs into specific classes according to conserved motives and their biosynthesized products (Segura et al., 2003; Srisawat et al., 2019; Busta et al., 2020; Wu et al., 2020).

OSCs are key enzymes that generate the large structural diversity of sterols and triterpenoids in nature (Wendt et al., 2000; Xu et al., 2004; Cárdenas et al., 2019). Here, sterols are originating from the common substrate 2,3-oxidosqualene via the initial formation of the protosteryl cation leading to products in "chair–boat–chair" conformation, whereas most triterpenoids are biosynthesized via the dammarenyl cation lead to products in "chair–chair–chair" conformation (Xue et al., 2012; Thimmappa et al., 2014; Cárdenas et al., 2019). Accordingly, dammarenyl cation-derived triterpenoids can be enzymatically converted into one or more of the triterpenoids saponin backbone structures. The formation is initiated by a protonation of the epoxide, via the aspartic acid in the DCTAE motif, which initiates a cascade of cyclization reactions and a deprotonation step leading to the final product (Figure 1; Hoshino and Sato, 2002; Ito et al., 2017). The cyclization results in products with one to five rings made of five to six carbons, referred to as the A, B, C, D, and E-rings with the A-ring being the first cyclized ring (Figure 1). To avoid the premature termination of cyclization, a number of aromatic residues serve to stabilize the intermediate carbocation by cation–π interactions, and by limiting the space for the substrate to change conformation (Thoma et al., 2004). Nevertheless, the differentiation of these OSC enzymes generating multiple products from sequence information remains difficult, especially amongst the classes of distinct and multifunctional β-amyrin synthases (Srisawat et al., 2019; Wu et al., 2020). Despite their high sequence similarity with exclusive β-amyrin synthases, these enzymes produce several dammarenyl cation-derived triterpenes (Morita et al., 2000; Moses et al., 2015; Wu et al.,

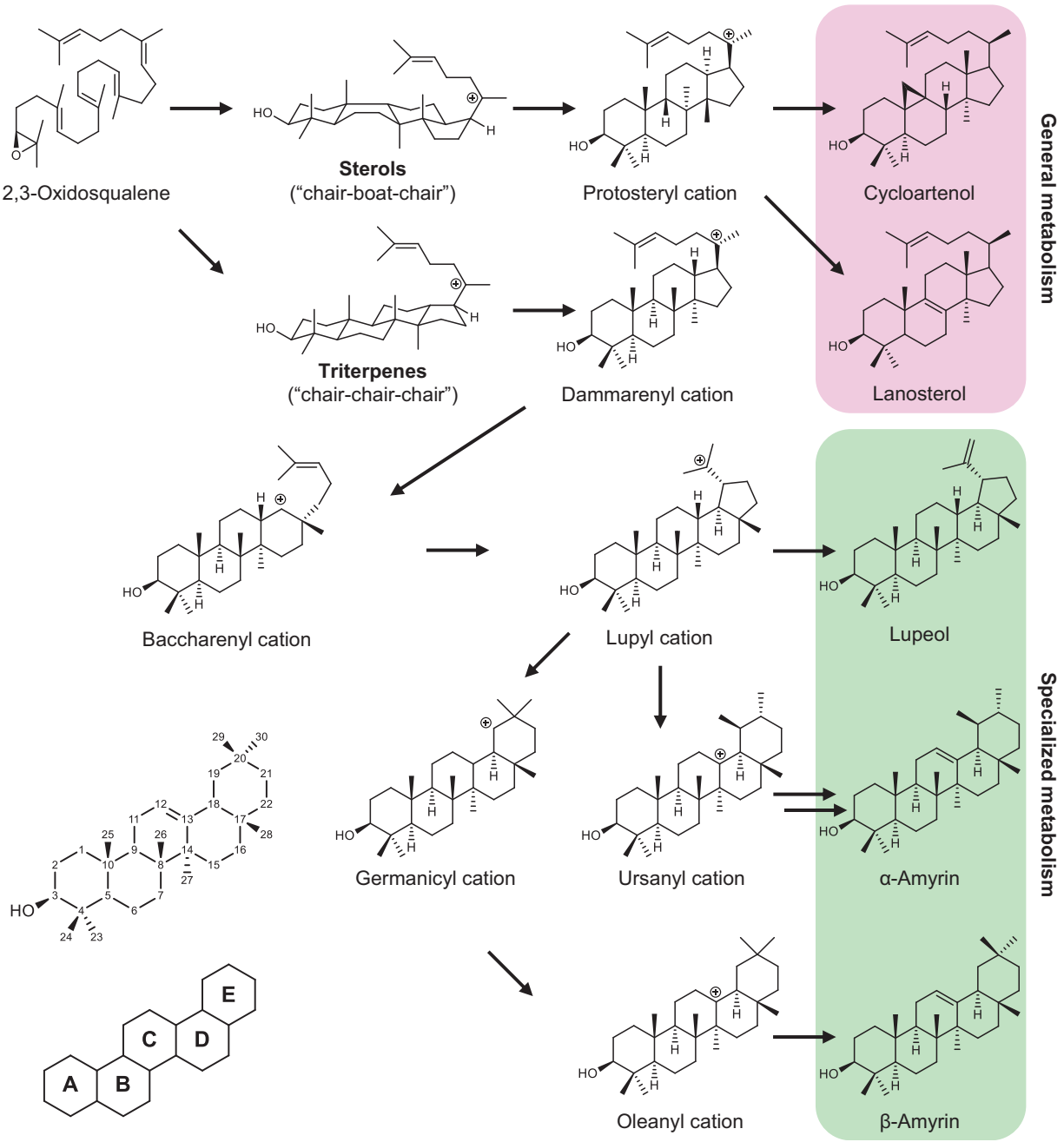

Figure 1 Biosynthesis of major plant triterpenoid backbones catalyzed by oxidosqualene cyclases. The shared precursor 2,3-oxidosqualene can undergo cyclization into the protosteryl cation in the "chair–boat–chair" conformation that gives rise to sterols like cycloartenol and lanosterol that are involved in general metabolism (lavender). Triterpenoids are derived from the dammarenyl cation in "chair–chair–chair" conformation and are involved in specialized metabolism (green). The dammarenyl cation can undergo ring expansion via the baccharenyl cation leadig to the formation of a large diversity of different cations that furthermore lead to diverse pentacyclic triterpenoids like. Enumeration of carbon atoms of the pentacyclic triterpenoid (β-amyrin) as well as ring identities of the corresponding pentacycle is shown in the left bottom.

2020). Here, α-amyrin, β-amyrin, and lupeol formation is initiated by protonation of 2,3-oxidosqualene. Concomitant cyclization yields the dammarenyl cation that undergoes proton transfer to result in baccharenyl cation formation, giving rise to the pentacyclic lupyl cation. The lupyl cation can deprotonate into lupeol. Depending on the steric hindrance of methyl group at C29 with cation–π interactions at the OSC active site residues, the lupyl cation can deprotonate into α-amyrin via the formation of the ursanyl cation (Xu et al., 2004). Alternatively, the lupyl cation can undergo ring expansion via C21 migration into the germanicyl cation and via further proton transfer to C13 forms the oleanyl cation. Deprotonation of the oleanyl cation results in the formation of β-amyrin or continue with further skeletal rearrangements (Thimmappa et al., 2014; Figure 1). Substantial efforts have been undertaken to

determine the reaction mechanism and unique structural features of multifunctional β-amyrin synthases in order to predict OSC function from sequence information (Segura et al., 2003; Ito et al., 2017; Srisawat et al., 2019; Wu et al., 2019, 2020).

In this study, we identified two amino acid residues that have a key role in the formation of both α-amyrin as well as β-amyrin. To narrow down the most prevalent effects of amino acid exchange, we generated hybrid constructs of P- and G-type *BvLUP5* and tested their function in plants by heterologous overexpression in *N. benthamiana*. To further define the catalytically relevant amino acids, we consecutively mutated single amino acids of G-type LUP5 in order to functionality recreate a mutant with P-type LUP5 catalytic activity and vice versa. Finally, we employed homology modeling to determine if the identified amino acid residues are close to the active center, and to identify if the amino acid residues have an impact on enzyme activity.

Results

Functional classification of plant OSCs reveals their preferred product formation

For the functional classification of the *B. vulgaris* LUP5s, we selected a set of previously characterized plant OSCs and performed a phylogenetic analysis (Figure 2). Based on functional characterization and main product formation reported in the literature, four classes of functionally different OSCs are highlighted in the phylogenetic analysis: multifunctional β-amyrin, β-amyrin, lupeol, or cycloartenol synthases (Salmon et al., 2016; Busta et al., 2020; Wu et al., 2020). For relating these catalytic functions with the amino acid sequences, we performed a multiple sequence alignment and highlighted conserved amino acid residues known to be involved in product specificity (Figure 2; Supplemental Table S1). The presence of His288 and Tyr571 are characteristic for OSCs involved in biosynthesis of cycloartenol (Wu et al., 2020). Characteristic for lupeol synthases is residue Leu-286, whereas differentiation between β-amyrin synthase and multifunctional β-amyrin synthase enzymes remains elusive from these sequence motifs. Both *B. vulgaris* OSC enzymes *Bv*LUP5-G and *Bv*LUP5-P grouped with the class of multifunctional β-amyrin synthases, which is in agreement with that they produce a mixture of β-amyrin, α-amyrin, and lupeol (Khakimov et al., 2015). A detailed amino acid alignment revealed conserved residues between the *Bv*LUP5-G and *Bv*LUP5-P enzymes as well as distinct amino acid changes within the *B. vulgaris* LUP5 enzymes were identified (Figure 3).

OSC chimeras narrow down the location of key amino acid residues involved in the α/β-amyrin product ratio

To determine amino acid residues involved in product formation, a set of chimeric genes of *Bv*LUP5-P and *Bv*LUP5-G (Chi1-4) were constructed. All chimeric enzymes consist of *Bv*LUP5-G with sequence substitutions of either the N-terminus (Chi1 and Chi2) or the C-terminus (Chi3 and Chi4) from *Bv*LUP5-P. The chimeric enzymes Chi1 and Chi2 have five and four amino acid residues substituted in the N-terminus, respectively (Figure 4A). *Bv*LUP5-P Chi3 and Chi4 have six amino acid residues substituted in the C-terminus. In addition, Chi4 has two mutations in the N-terminus, due to homologous recombination of the N-terminus of *Bv*LUP5-G with a contamination of an N-terminal fragment from *BvLUP5-P* in the PCR reaction. The chimeric constructs were heterologously expressed in *N. benthamiana* leaves and metabolites were extracted and analyzed by gas chromatography–mass spectroscopy. The chimeric enzymes generated the shared *Bv*LUP5 products β-amyrin, α-amyrin, and lupeol in different ratios, indicating that the activities of the different chimeric enzymes differ (Figure 4B; Supplemental Figure S1). *Nicotiana benthamiana* plants overexpressing the candidate genes did not produce new triterpenoid metabolites; however, the product ratios differed significantly between the overexpressed chimeric genes (Supplemental Table S2). The total product amount of α-amyrin, β-amyrin, and lupeol of the wild-type and chimeric LUP5 expression constructs was analyzed to compare effects on product accumulation and normalized to the combined peak areas. For the ratio calculations, the minor product lupeol was omitted from the ratio calculations as the amount was negligible compared to α-amyrin and β-amyrin. Of the four chimeras, Chi3 and Chi4 had a product ratio least similar to *Bv*LUP5-G. The β-amyrin to α-amyrin ratio of Chi3 approximates one and is therefore comparable to neither *Bv*LUP5-P nor *Bv*LUP5-G product ratios. Chi4 produced 41% β-amyrin and 55% α-amyrin, which are comparable to the *Bv*LUP5-P product profile of 35% β-amyrin and 61% α-amyrin (Figure 4; Supplemental Table S2). Chi3 differs from Chi4 by only three amino acid residues, underpinning the minor importance of amino acid residues 418, 435, and 453 for determining the product ratio between α- and β-amyrin. Additionally, Chi1 and Chi2 do not result in a different β-amyrin to α-amyrin ratio; however, the total activity of these chimeras seems to be reduced in vivo in comparison to *Bv*LUP5-G, suggesting that these portions of the protein might contribute to the stability of the enzyme but not on the catalysis. These results suggest that the C-terminal part of the *Bv*LUP5-G is crucial for the biosynthesis of a larger ratio of β-amyrin to α-amyrin.

Reciprocal mutagenesis identifies amino acids involved in major product formation of *B. vulgaris* LUP5

Next, we investigated the effects of single and multiple amino acid changes within both *Bv*LUP5 enzymes to identify crucial amino acids for the generation of β-amyrin and α-amyrin, respectively. For the chimeric construct, we observed considerable differences in the overall product accumulation. Amongst the reciprocal mutations, single amino acid exchanges showed relatively little effects on product ratio alteration, while multiple changes showed bigger effects

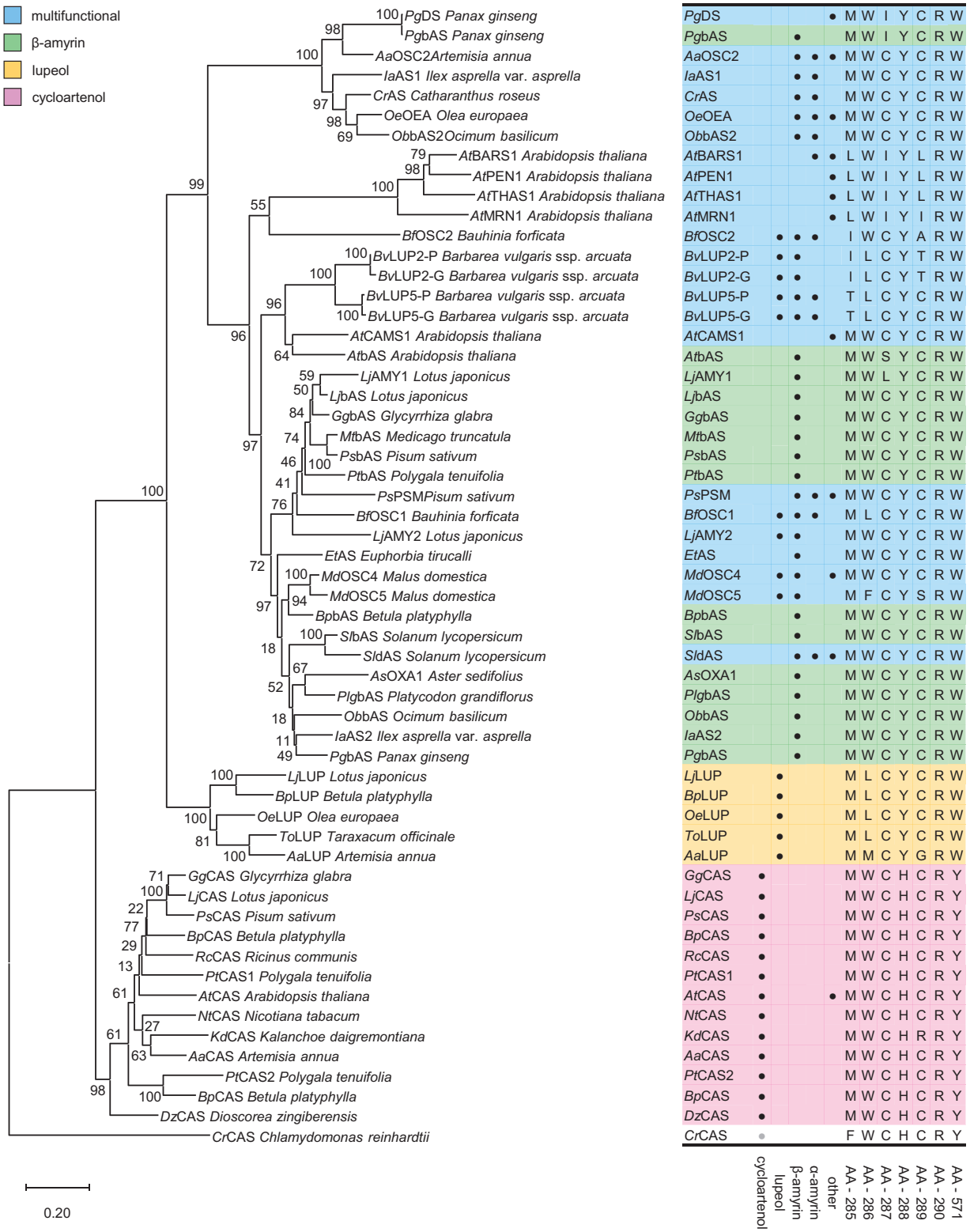

Figure 2 Phylogenetic analysis combined with sequence features of charachterized plant OSCs. Plant OSCs can be functionally grouped into cycloartenol synthases (lavender), lupeol synthases (yellow), β-amyrin synthases (green), and multifunctional amyrin synthases (blue). The functionally uncharacterized (gray dot), predicted cycloartenol synthase from *C. reinhardtii* was used as a root. Corresponding to the phylogeny, sequence identifiers and biosynthesized triterpenoid products are shown (black dot) together with key conserved amino acid residues. Evolutionary history was inferred by the maximum likelihood statistical method with MEGA-X. The phylogenetic tree with the highest log likelihood (−32,372.53) is shown. Distances were computed using the JTT matrix-based method. The phylogenetic tree was constructed using 1,000 bootstrap replicates. The percentage of trees in which the associated taxa clustered together is shown next to the branches. The scale bar shows the branch length representing 0.2 amino acid substitutions per site.

(Figure 5). In both approaches, the amino acids at position 735 and 740 had the strongest effect on product ratio. The amino acid mutations A121T, Q418L, L735I, F740Y and S98A, A121T, L735I, F740Y of *Bv*LUP5-G resulted in product ratios and relative activities highly similar to *Bv*LUP5-P (Figure 5A; Supplemental Figure S2). Conversely, the mutations of the residues T121A, I735L and T121A, F170V, I735L of *Bv*LUP5-P were sufficient to render the product profile and relative activity similar to *Bv*LUP5-G (Figure 5B; Supplemental Figure S3). In both cases, the interconversion of the amino acid residues at position 121, 735, and 740 were concluded to be crucial for converting the primarily β-amyrin producing *Bv*LUP5-G to the primarily α-amyrin producing *Bv*LUP5-P and vice versa. However, single mutation of residue 740 did not substantially alter the product ratio in neither *Bv*LUP5-G nor *Bv*LUP5-P. Taken together, these results suggest, that the amino acids at the positions 121 and 735 are primarily influencing both product ratio as well as relative activity of *B. vulgaris* LUP5 enzymes. This effect appears more pronounced when these residues are reciprocally mutated together (Figure 5).

Structural homology modeling substantiates involvement of amino acids 121 and 735 in shifts of α/β-amyrin product ratios

To see where reciprocally changed amino acids are situated in the enzyme, we generated homology models of the *Bv*LUP5-G and *Bv*LUP5-P using human lanosterol synthase (LAS; PDB identifier: 1W6K) as a template (Thoma et al., 2004). In order to gain insights into the close interactions of the products with the enzyme active center, we employed computational docking of the main products β-amyrin and α-amyrin (Figure 6). Indeed, molecular docking with the products β-amyrin and α-amyrin substantiated the experimentally determined residues involved in product formation. All amino acid residues that differ between the two *Bv*LUP5 enzymes are highlighted (Figure 3) and specific features of their side-chain, their position in the homology model as well as their secondary structure are annotated (Supplemental Table S3). Amino acid residue 121 locates close to the active center and the initiation site, which could explain the findings in our mutagenesis studies. Amino acid residues 735 and 740 directly point toward the active center. Amino acid residue 735 is positioned between the active center and amino acid residue 121, suggesting their interaction with the reactive intermediate and the product. Nevertheless, amino acid 121 possibly contributes to the correct positioning of residue 735 via steric hindrance and thus pushes this residue closer into the active site. Amino acid residue 740 locates close to the interface of the side-channel and the active center, suggesting potential interaction with the DCTAE motif and involvement in catalysis.

Discussion

We have showed that the formation of insecticidal saponins within species of the *Barbarea* complex are dependent on

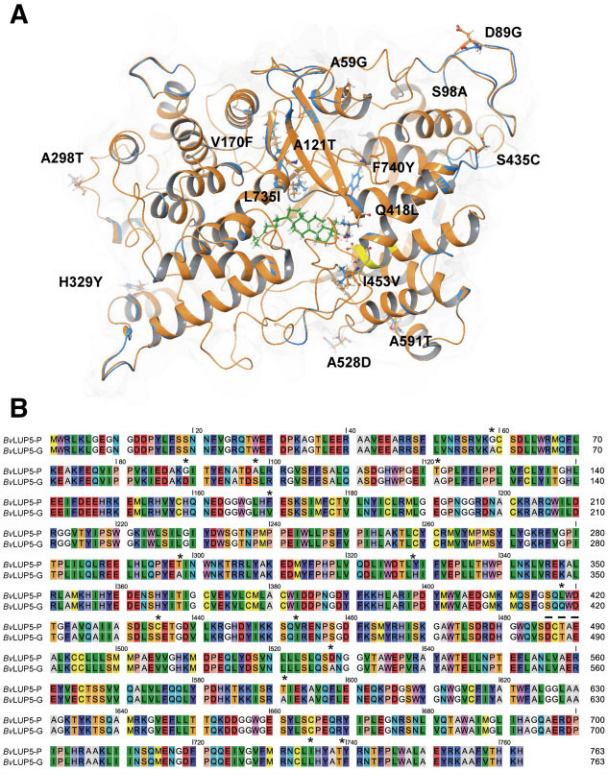

Figure 3 Structural comparison of BvLUP5-G and BvLUP5-P. Overlay of homology models of BvLUP5-G and BvLUP5-P (A). Amino acids that differ between the two structures are marked as sticks. Orange: BvLUP5-G; Blue: BvLUP5-P; Yellow: DCTAE motif; Green: Lanosterol. Amino acid alignment of BvLUP5-G and BvLUP5-P (B). Asterisk denotes nonidentical amino acids. Reciprocally mutated amino acids are highlighted by an asterisk. Active center motif DCTAE is highlighted with a dashed line.

the formation of a β-amyrin-derived triterpenoid backbone (Khakimov et al., 2015; Byrne et al., 2017; Erthmann et al., 2018; Liu et al., 2019). β-amyrin production could be assigned to the LUP5 gene in both G- and P-type *B. vulgaris* (Khakimov et al., 2015; Byrne et al., 2017); however, these genes are differentially expressed with LUP5 being expressed 10-fold higher in the G-type as compared to the P-type (Khakimov et al., 2015). Furthermore, G- and P-type LUP5 enzymes show a difference in the product ratio between α-amyrin and β-amyrin, where the β-amyrin/α-amyrin is 10-fold higher in the G-type than in the P-type. Combined, the difference in expression level of the LUP5 genes and in the product ratio determines that insecticidal β-amyrin-derived saponins are prevalent in the G-type and minute in the susceptible P-type (Khakimov et al., 2016). Thus, our aim was to identify the amino acid residues in *Bv*LUP5 enzymes that determine the product ratio of α-amyrin and β-amyrin via reciprocal mutation and homology modeling.

We identified several shared common features of *B. vulgaris* LUP5 enzymes with other known plant multifunctional β-amyrin synthases via amino acid sequence comparison (Figure 2; Supplemental Table S1) and located 14 specific amino acid changes that differ between *Bv*LUP5-P and

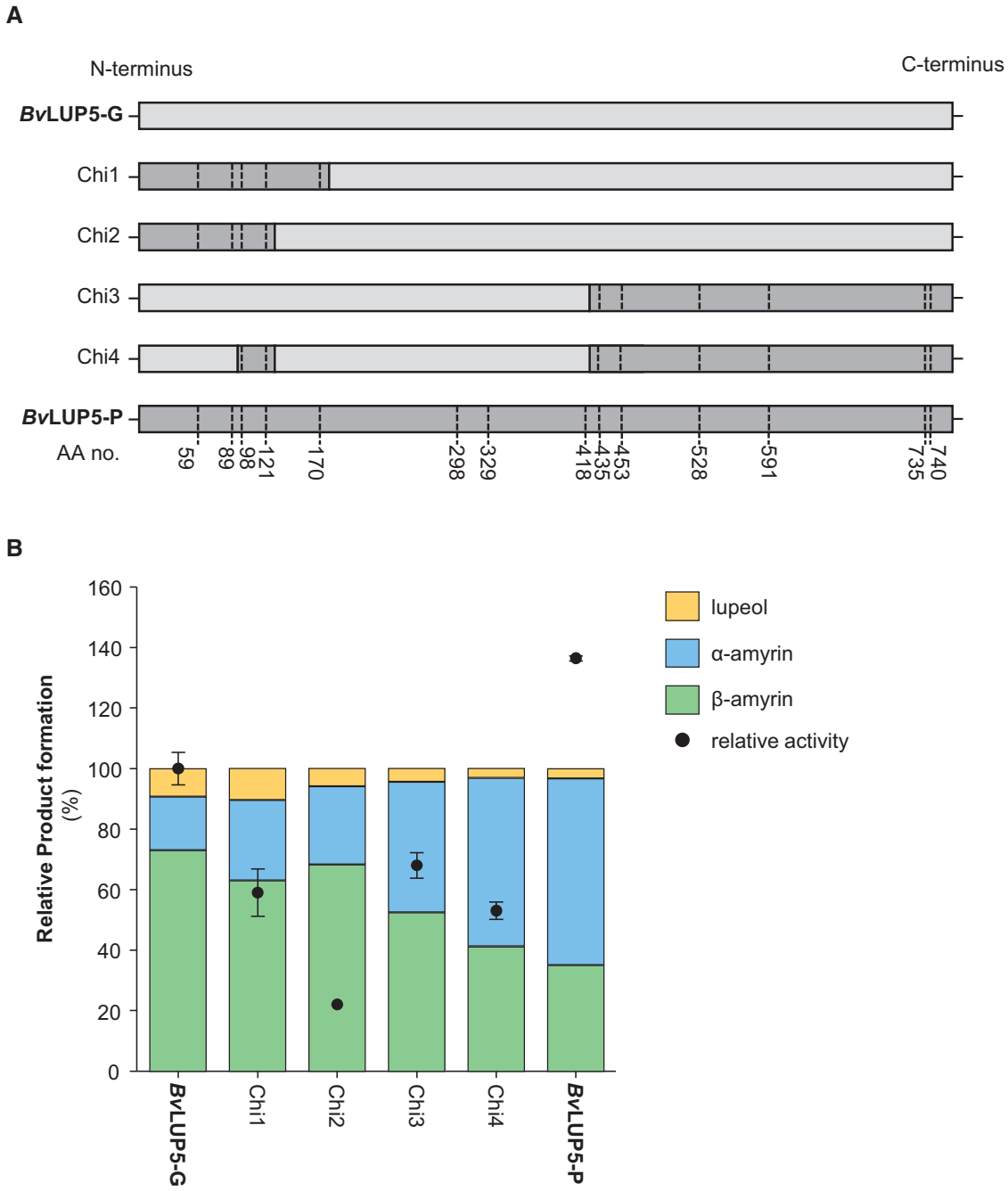

Figure 4 Engineered chimeric products of *Bv*LUP5 generate altered product profiles. Different domains of *Bv*LUP5-G and *Bv*LUP5-P harbor specific amino acid alterations (A). Product profiles composed of β-amyrin, α-amyrin, and lupeol of the wild-type and chimeric LUP5 expressing *N. benthamiana* lines (B). Relative enzyme activity is visualized as dots. Mean ± SD are shown (n = 3).

*Bv*LUP5-G (Figure 3). Heterologous expression of *BvLUP5-G* and *BvLUP5-P* in *N. benthamiana* leaves confirmed their multiproduct formation of β-amyrin, α-amyrin, and lupeol in different ratios (Figures 4 and 5). As described earlier, the overexpression of *BvLUP5-P* resulted primarily in the accumulation of α-amyrin, and the overexpression of *BvLUP5-G* resulted primarily in the accumulation of β-amyrin (Khakimov et al., 2015; Figure 5). Due to the high evolutionary relatedness of OSC enzymes in general, high sequence conservation is expected to resemble functional similarities (Lodeiro et al., 2004; Salmon et al., 2016; Busta et al., 2020; Wu et al., 2020). Our data indicate that the exchange of domains located close to the C-terminus of *Bv*LUP5-G was most associated with altered product ratios (Figure 4; Supplemental Table S2), suggesting an indirect interaction with the DCTAE motif. Essentially, when the C-terminus and the N-terminus of *Bv*LUP5-G was replaced with the C-terminus and N-terminus from *Bv*LUP5-P, the ratio of accumulating α-amyrin increased in comparison to the wild-type (Figure 4). Furthermore, when the N-terminus was

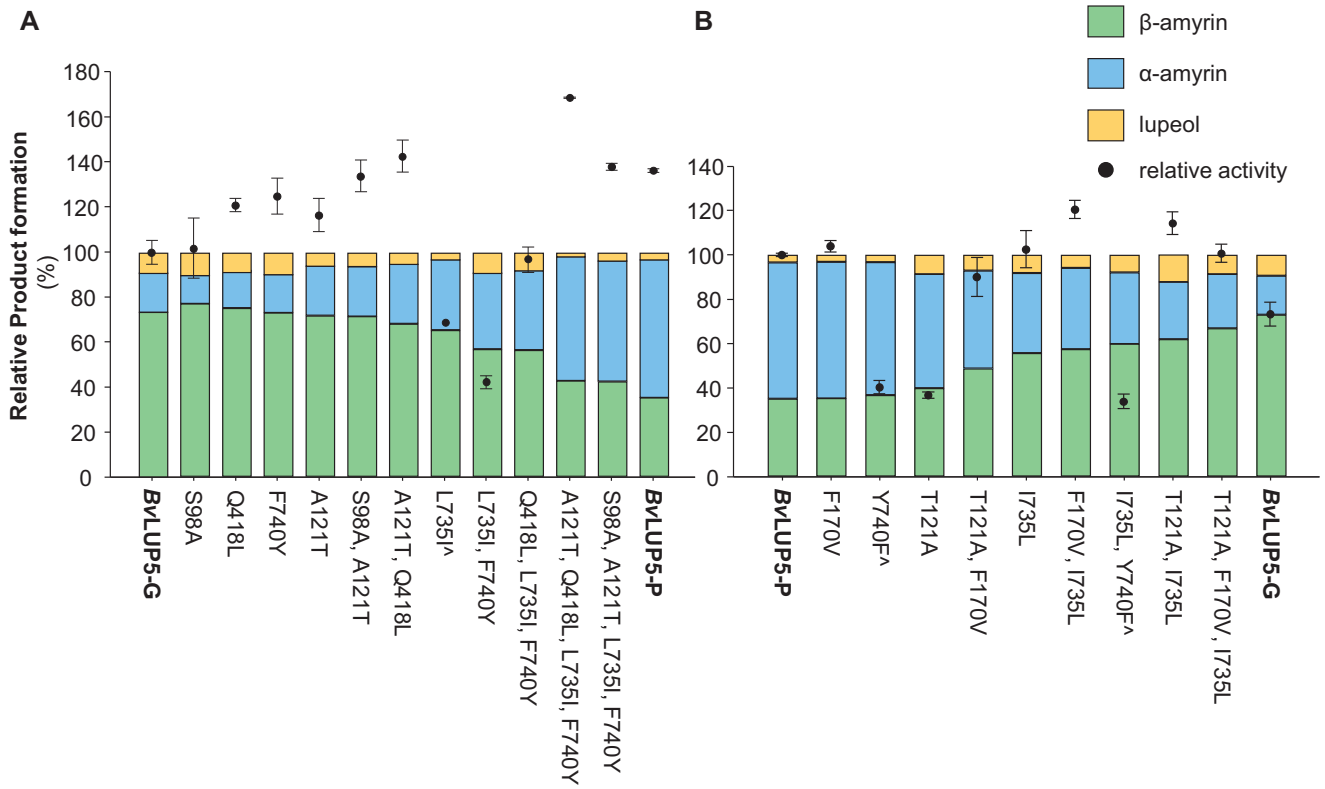

Figure 5 Product profiles and relative activity of the wild-type and mutant LUP5 expressing *N. benthamiana* lines. Partial reciprocal mutagenesis of *Bv*LUP5-G generates *Bv*LUP5-P product profiles and relative activity (A) and vice versa (B). Relative enzyme activity is visualized as dots. Mean ± SD are shown (n = 3).

exchanged, the product ratios remained similar to the wild-type *Bv*LUP5-G, suggesting that the C-terminal region harbors amino acid changes that dominantly altered the product ratio (Figure 4). Indeed, the amino acid residues affected in these mutants have been localized close to the active center residues that were shown to affect the product ratio of multifunctional β-amyrin synthase enzymes (Salmon et al., 2016; Busta et al., 2020; Wu et al., 2020). However, the mutational changes could not account for the complete product switch and similar relative activity of *Bv*LUP5-G to *Bv*LUP5-P, suggesting that synergistic effects of amino acids within different domains might contribute to the product specificity of multifunctional β-amyrin synthases of *B. vulgaris*.

Therefore, we carried out further detailed mutational studies altering single, double, or multiple amino acid residues of *Bv*LUP5-P and *Bv*LUP5-G to interconvert their enzymatic activities via reciprocal mutagenesis. Indeed, our observations could further be validated by mutating single amino acid residues. The site-directed mutagenesis advocated amino acid residue Thr121 and Leu735 as the major contributors to the observed change in product ratio (Figure 5). However, Thr121 does not directly reach into the active site but likely contributes to the positioning of the Leu735 (Figure 3A). Tyr740 is in close proximity to the active center; however, single-point mutation of this amino acid residue did not change product ratio in the corresponding *Bv*LUP5-P or *Bv*LUP5-G mutants. The increased α/β-amyrin product ratio generated by the mutant A121T, Q418L, L735I, F740Y compared to the wild-type *Bv*LUP5-G is due to the larger steric properties of threonine instead of alanine. Presumably, threonine at position 121 pushes the isoleucine sidechain from 735 into the active site, which overall affects the binding pocket so the ursanyl cation is preferred rather than the oleanyl cation. In contrast, the *Bv*LUP5-P mutant F170V, T121A, I735L influences the spatial position of the side-chains of amino acid residue 121 and 735, which favors the oleanyl cation rather than the ursanyl cation; however, the exact mechanism remains to be identified. Mutation of amino acid residue 121 in either *Bv*LUP5-G or *Bv*LUP5-P resulted in a total product amount of 117% or 37%, respectively (Figure 5; Supplemental Table S2). Therefore, the amino acid at position 121 is likely involved in the formation of one of the initial cations. Introduction of a threonine at position 121 in *Bv*LUP5-P, instead of the alanine present in *Bv*LUP5-G increased the overall product amount (Figure 5; Supplemental Table S2). The threonine is located in close proximity of the aliphatic residue at position 735, suggesting that the amino acid at this position is involved in stabilizing residues within the active site or altering the space within the active site. Additionally, these results further substantiate our earlier observations suggesting synergistic effects of amino acid residues located in different domains. Furthermore, tyrosine at position 740

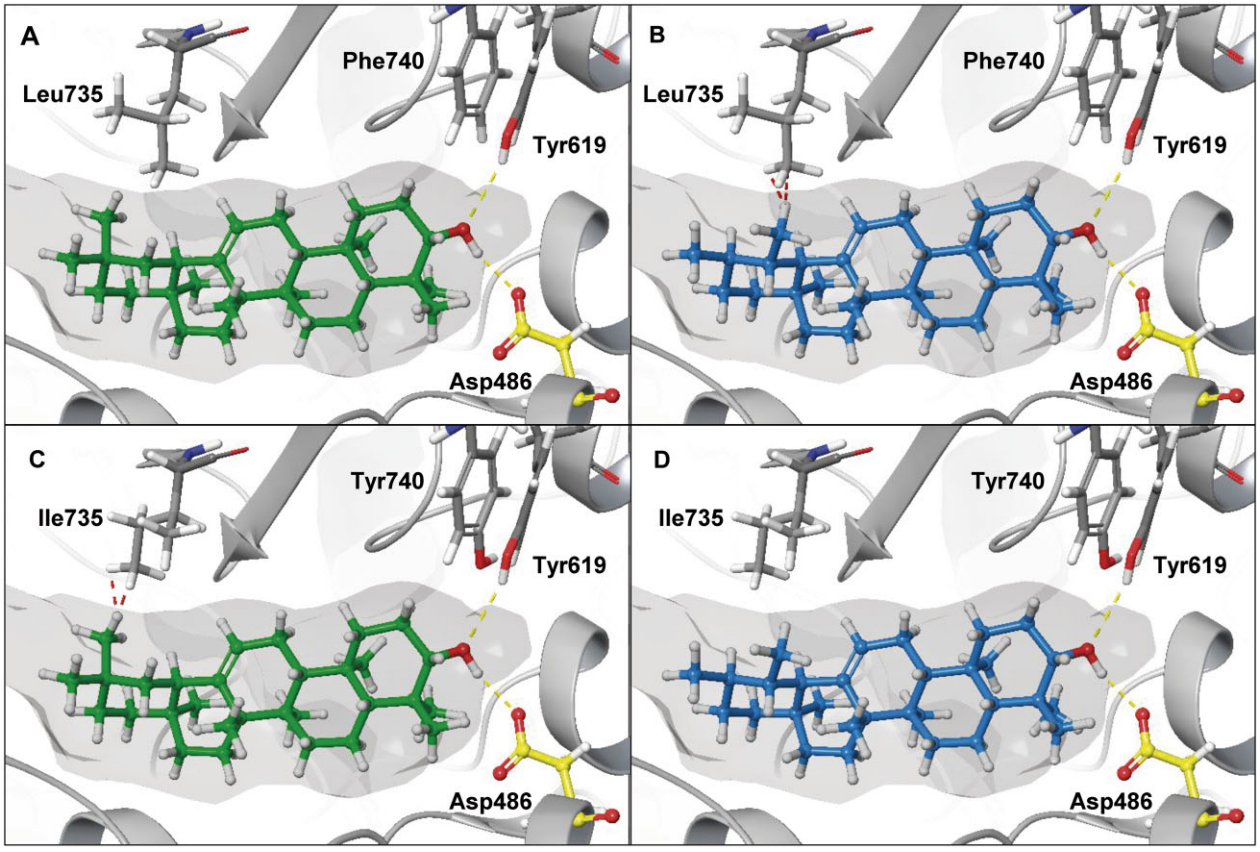

Figure 6 Molecular modeling and docking studies support the distinct catalysis of *Bv*LUP5-G in comparison to *Bv*LUP5-P. Active center architectures of *Bv*LUP5-G (A and B) and *Bv*LUP5-P (C and D) with docked biosynthesized products β-amyrin (green) and α-amyrin (blue). The common substrate pocket is shown in light grey. Important amino acid residues are represented as ball and stick. Severe steric clashes between the substrates and enyzme are highlighted as red dotted lines. Beneficial hydrogen bonding with Asp486 (yellow) of the DCTAE motif and Tyr619 are highlighted as yellow dotted lines.

is highly conserved in numerous OSCs, suggesting major importance of this residue in triterpene formation. In our model, amino acid residue 740 is located in close proximity to the DCTAE motif. Potentially, tyrosine could form a hydrogen bond with the hydroxyl group of Tyr619 that is involved in the coordination of the 3OH group of the triterpenoid substrate, thereby increasing the acidity of this residue. In concert with Asp486 of the DCTAE motif both residues are likely contributing to the correct coordination of the substrate within the active site throughout catalysis. The double mutation L735I, F740Y, or I735L, Y740F decreased the product amount to the lowest levels observed for the two OSC enzymes (42% and 32% for *Bv*LUP5-G and *Bv*LUP5-P, respectively; Figure 5; Supplemental Table S2), and also affected the product ratio more than any single mutation. We suggest this change is caused by the side-chain combination of I121 and Y740, which affects the conformation of the initiation site, possibly due to the substrate and initiation site being pushed apart. This may explain the decrease in product observed when mutating only L735I. Additionally, the product amount is further decreased when adding the mutation F740Y. Here, the isoleucine changes the conformation of the initiation site by pushing the substrate and initiation motif away from each other, which is further distanced by the introduced tyrosine hydroxyl group. Indeed, it has been shown that tyrosine in this position is important for stabilization of the A and B ring formation of triterpenoids (Racolta et al., 2012). In our modeling study, the combination of Ile735 and Tyr740 seems sterically hinder the methyl group on C29 due to weaker coordination of the 3OH group that pushes the C29 methyl group out of the binding site and even closer towards Ile735 (Figure 6). Therefore, specifically β-amyrin is repulsed from Isoleucine towards the opposing active site boundary. Therefore, the Me29 and Me30 groups are sterically less favorable to form from the corresponding precursor cations. However, when the α-amyrin formation is favored, isoleucine is not as detrimental for the product formation as the hydrophobic bulk from the methyl groups is evenly spread among the α-amyrin molecule (at C19 and C20) and thus does not lead to an equally strong hydrophobic repulsion from Ile735. Our modeling data show that the binding of α-amyrin in the active center of *Bv*LUP5-P and the binding of β-amyrin in the active center of *Bv*LUP5-G represent less steric clashes (Figure 6, A and D). Additionally, it has been suggested that optimal results are obtained when using

both transition states as well as final reaction products that for molecular docking (Wu et al., 2020). For example, the model of *Bv*LUP5-P showed highest docking scores for α-amyrin as well as for the intermediates leading to the formation of α-amyrin. Interestingly, the residues investigated to be largely at play in determining the product ratio in *B. vulgaris* LUP5 enzymes, were not reported previously to determine product ratios in multifunctional β-amyrin synthases. However, several different architecture have been described for OSC enzymes found in plants catalyzing similar reactions (Srisawat et al., 2019; Wu et al., 2019, 2020). Taken together, these biosynthetic mechanisms are dictated by the OSC active center environment, determining the stability of cationic intermediates and correct positioning of the intermediate in order to facilitate product formation (Ito et al., 2013, 2017). However, these reactions can be catalyzed by different active site architecture, allowing for several different ways for the generation of the same product, which is also apparent from the phylogenetic analysis in Figure 2. Indeed, convergent evolution has been observed commonly in plant specialized metabolism in general (Pichersky and Lewinsohn, 2011) and by OSCs (Cárdenas et al., 2019).

In nature, the occurrence of multifunctional OSCs allows for a multitude of intermediates which suggests that OSC catalysis might undergo large spectra of catalytic reactions (Lodeiro et al., 2007). Therefore, it has been argued that nature explores functional sequence space of OSC cyclization via single mutations (Salmon et al., 2016). Here, we showed that despite the frequent accumulation of mutations in OSC enzymes within the *Barbarea* complex, only few mutations drastically alter the product ratio. In an evolutionary perspective, a large diversity of generated triterpenoids is a key factor that contributes to the biosynthetic capacity of a plant to continuously mount an effective anti-herbivore defense (Khakimov et al., 2015; Byrne et al., 2017). It has been proposed that, promiscuous multifunctional enzymes like OSCs point toward evolutionarily young stage of biochemical pathways (Aharoni et al., 2005; Moghe and Last, 2015; Moghe et al., 2017). Indeed, several examples have shown that enzymes that initiate the biosynthesis of specialized defense metabolites are highly promiscuous (Leong and Last, 2017). Here, we have shown that few mutations are sufficient to alter triterpene product ratios. We suggest that these alterations enable the channeling of triterpene precursors into further biosynthetic modifications and lead to a diversification of potential bioactive products that can be employed for plant defense (Jones and Vogt, 2001; Hamberger and Bak, 2013). Therefore, *B. vulgaris* LUP5s are kept in a transition state possibly enabling highly dynamic adaptations within plant specialized metabolism throughout evolutionary trajectories. Surprisingly, the identified OSC mutations do not alter the generated triterpene diversity but the product ratio. These results suggest that the increased biosynthesis of β-amyrin over α-amyrin might lead to the increased substrate supply for further modification steps via P450 and UGT enzymes that further convert β-amyrin into saponins that act as potent defense metabolites in *B. vulgaris* (Khakimov et al., 2015; Erthmann et al., 2018; Liu et al., 2019). The naturally occurring mutations within *BvLUP5* genes likely contribute to the generation of insecticidal saponins in G-Type *B. vulgaris* plants in contrast to P-type plants. Therefore, the *B. vulgaris* complex represents a unique model to study the evolution of specialized metabolite pathways that contribute to plant defense.

Materials and methods

Phylogeny and amino acid alignment

OSC cDNA sequences were retrieved from GeneBank and used for an amino acid alignment (Supplemental Table S1). Amino acid sequence alignments were constructed with the ClustalW (codon) algorithm (pairwise alignment: gap open, 10; gap extend, 0.1; multiple alignment: gap open, 10; gap extend, 0.2) implemented in the software MEGA-X (Kumar et al., 2018). The phylogenetic tree was generated with MEGA-X using the Maximum Likelihood method performing 1,000 bootstrap replicates (Jones–Taylor–Thornton model; Jones et al., 1992). Substitution type, amino acid; rates among sites, gamma distributed (+ G, parameter = 1.1878) with invariant sites ([+ I], 4.72% sites); gaps/missing data treatment, use all sites; site coverage cutoff, 95%). For visualization of characteristic enzyme functionalities, primarily generated reaction products are listed (Supplemental Table S1).

Cloning and transformation

Point mutations were introduced into wild-type sequences of *B. vulgaris* *Bv*LUP5-P and *Bv*LUP5-G by PCR inspired by Zheng et al. (2004) using primers (Supplemental Table S4). PCR program: 98°C; 30 s, 30 cycles of 98°C; 10 s, 62°C; 30 s, 72°C; 3 min followed by final extension of 72°C; 10 min. X7 polymerase was used for the PCR reactions (Nørholm, 2010). After PCR the nonmutated amplicons were digested with restriction enzyme *DpnI* according to manufactures instructions (New England Biolabs). If several mutations were required, additional PCRs were performed. Primers are listed in Supplemental Table S4. Chimeric genes were designed by amplifying either N-terminal, middle part or C-terminal by PCR followed by gel purification, before combining these parts as templates in a new PCR reaction. All constructs were cloned using the gateway system following manufactures protocol (Invitrogen) using pDONR207 (Invitrogen) and pEAQ-HT-DEST1 (Sainsbury et al., 2009) prior to transient expression in tobacco (*N. benthamiana*) leaves.

Expression in *N. benthamiana*

Constructs were transformed into *Agrobacterium tumefaciens* strain AGL1 or LBA4404. One colony was plated onto LB media agar plates and after 2 d of incubation one loop full of colonies were transferred into 10 mL LB media and incubated 28°C O/N at 220 rpm. The following day the cultures were centrifuged at 5,163 rpm 10 min to pellet the

cells. Cells were resuspended into buffer (10-mM $MgCl_2$, 10-mM MES, 100-μM acetosyringone, pH 5.6) to obtain an optical density $(OD)_{600}$ of app. 0.5. Suspensions were incubated 3 h at room temperature before infiltration into *N. benthamiana* leaves. Three-week-old *N. benthamiana* plants were grown in 25°C with a photoperiod of 16 h of day light. The youngest fully developed leaf was used for infiltration, and for each construct, three plants were infiltrated.

Metabolite extraction

Leaf discs (1.5-cm diameter) were harvested from each infiltrated leaf, placed in a 2 mL tube and flash frozen in liquid nitrogen. To each tube, 500-μL ethyl acetate with 33.3 μM of betulinic acid (internal standard) were added and samples were incubated 3 h at room temperature (~25°C) with slow agitation.

GC–MS and data analysis

GC–MS analysis were performed as previously described (Khakimov et al., 2013), and data processed by the PARAFAC2 method (Khakimov et al., 2012). Peaks were identified by comparing retention times and fragmentation patterns with standards; β-amyrin, α-amyrin, and lupeol all from Sigma-Aldrich. Relative concentrations of metabolites were normalized by division of each peak area by the sum of all peak areas detected in the sample. Outliers were removed before the calculations of the ratios and the ANOVAs and are marked with " ^" in Supplemental Table S2. The abundance of β-amyrin, α-amyrin, and lupeol were calculated by dividing the normalized relative concentration of each compound with the sum of normalized relative concentrations from all three compounds.

Homology modeling

Homology modeling was carried out using Schrödinger Maestro 12.7 (Schrödinger Release 2021-1: Maestro, Schrödinger, LLC, New York, NY, 2021.). Protein models were based on the human lanosterol cyclase (LAS) as template (PDB ID: 1W6K; Thoma et al., 2004). Alignments and secondary structure predictions were performed with CLC main workbench 20.0.4 (Qiagen).

Accession numbers

Sequence data from this article can be found in the GenBank/EMBL data libraries under accession numbers KP784690.1 (*BvLUP5-G*) and KP784689.1 (*BvLUP5-P*).

Supplemental data

The following materials are available in the online version of this article.

Supplemental Figure S1. Engineered chimeric *BvLUP5* product profiles.

Supplemental Figure S2. Representative mean GC–MS product profiles of engineered single amino acid mutants of *Bv*LUP5-G.

Supplemental Figure S3. Representative mean GC–MS product profiles of engineered single amino acid mutants of *Bv*LUP5-P.

Supplemental Table S1. Amino acid alignment of characterized plant oxidosqualene cyclases.

Supplemental Table S2. Product profiles of reciprocally mutated *Bv*LUP5-P and *Bv*LUP5-G.

Supplemental Table S3. Amino acid residues that differ between BvLUP5-P and BvLUP5-G (one letter code).

Supplemental Table S4. Primers used in this study.

Supplemental Material. Structural coordinates of modelled *Bv*LUP5-G and *Bv*LUP5-P.

Acknowledgments

We thank the European Community's Seventh Framework Programme (FP7/2007-2013; grant no. 613692 to TriForC) for supporting this work. We thank Pablo D. Cárdenas and Nils Agerbirk for thorough reading and constructive input during writing of this manuscript.

Funding

This work was funded by The Danish Council for Independent Research, Technology and Production Sciences (grant no. 1335-00151), the Novo Nordisk Foundation, Distinguished Investigator (grant no. NNF20OC0060298), and Department of Plant and Environmental Sciences, University of Copenhagen (PhD stipend to PØE).

Conflict of interest statement. The authors declare no conflict of interest.

References

Agerbirk N, Olsen CE, Bibby BM, Frandsen HO, Brown LD, Nielsen JK, Renwick JAA (2003) A saponin correlated with variable resistance of Barbarea vulgaris to the diamondback moth Plutella xylostella. J Chem Ecol **29**: 1417–1433

Aharoni A, Gaidukov L, Khersonsky O, Gould SMQ, Roodveldt C, Tawfik DS (2005) The "evolvability" of promiscuous protein functions. Nat Genet **37**: 73–76

Augustin JM, Kuzina V, Andersen SB, Bak S (2011) Molecular activities, biosynthesis and evolution of triterpenoid saponins. Phytochemistry **72**: 435–457

Badenes-Perez FR, Gershenzon J, Heckel DG (2014) Insect attraction versus plant defense: Young leaves high in glucosinolates stimulate oviposition by a specialist herbivore despite poor larval survival due to high saponin content. PLoS One **9**: 39–42

Busta L, Serra O, Kim OT, Molinas M, Peré-Fossoul I, Figueras M, Jetter R (2020) Oxidosqualene cyclases involved in the biosynthesis of triterpenoids in Quercus suber cork. Sci Rep **10**: 1–12

Byrne SL, Erthmann PØ, Agerbirk N, Bak S, Hauser TP, Nagy I, Paina C, Asp T (2017) The genome sequence of Barbarea vulgaris facilitates the study of ecological biochemistry. Sci Rep **7**: 1–14

Cárdenas PD, Almeida A, Bak S (2019) Evolution of structural diversity of triterpenoids. Front Plant Sci **10**: 1–10

Chen YF, Yang CH, Chang MS, Ciou YP, Huang YC (2010) Foam properties and detergent abilities of the saponins from Camellia oleifera. Int J Mol Sci **11**: 4417–4425

Christensen S, Enge S, Jensen KR, Müller C, Kiær LP, Agerbirk N, Heimes C, Hauser TP (2019) Different herbivore responses to two

co-occurring chemotypes of the wild crucifer Barbarea vulgaris. Arthropod Plant Interact **13**: 19–30

Christensen S, Heimes C, Agerbirk N, Kuzina V, Olsen CE, Hauser TP (2014) Different geographical distributions of two chemotypes of Barbarea vulgaris that differ in resistance to insects and a pathogen. J Chem Ecol **40**: 491–501

Erthmann PØ, Agerbirk N, Bak S (2018) A tandem array of UDP-glycosyltransferases from the UGT73C subfamily glycosylate sapogenins, forming a spectrum of mono- and bisdesmosidic saponins. Plant Mol Biol **97**: 37–55

Hamberger B, Bak S (2013) Plant P450s as versatile drivers for evolution of species-specific chemical diversity. Philos Trans R Soc B Biol Sci **368**: 20120426.

Haralampidis K, Bryan G, Qi X, Papadopoulou K, Bakht S, Melton R, Osbourn A (2001) A new class of oxidosqualene cyclases directs synthesis of antimicrobial phytoprotectants in monocots. Proc Natl Acad Sci USA **98**: 13431–13436

Hauser TP, Toneatto F, Nielsen JK (2012) Genetic and geographic structure of an insect resistant and a susceptible type of Barbarea vulgaris in western Europe. Evol Ecol **26**: 611–624

Hoshino T, Sato T (2002) Squalene-hopene cyclase: Catalytic mechanism and substrate recognition. Chem Commun **2**: 291–301

Ito R, Masukawa Y, Hoshino T (2013) Purification, kinetics, inhibitors and CD for recombinant β-amyrin synthase from Euphorbia tirucalli L and functional analysis of the DCTA motif, which is highly conserved among oxidosqualene cyclases. FEBS J **280**: 1267–1280

Ito R, Nakada C, Hoshino T (2017) β-Amyrin synthase from Euphorbia tirucalli L. functional analyses of the highly conserved aromatic residues Phe413, Tyr259 and Trp257 disclose the importance of the appropriate steric bulk, and cation-π and CH-π interactions for the efficient catalytic ac. Org Biomol Chem **15**: 177–188

Jiang X, Cao Y, von Gersdorff L, Strobel BW, Hansen HCB, Cedergreen N (2018) Where does the toxicity come from in saponin extract? Chemosphere **204**: 243–250

Jones DT, Taylor WR, Thornton JM (1992) The rapid generation of mutation data matrices from protein sequences. Bioinformatics **8**: 275–282

Jones P, Vogt T (2001) Glycosyltransferases in secondary plant metabolism: tranquilizers and stimulant controllers. Planta **213**: 164–174

Khakimov B, Amigo JM, Bak S, Engelsen SB (2012) Plant metabolomics: Resolution and quantification of elusive peaks in liquid chromatography-mass spectrometry profiles of complex plant extracts using multi-way decomposition methods. J Chromatogr A **1266**: 84–94

Khakimov B, Kuzina V, Erthmann P, Fukushima EO, Augustin JM, Olsen CE, Scholtalbers J, Volpin H, Andersen SB, Hauser TP, et al. (2015) Identification and genome organization of saponin pathway genes from a wild crucifer, and their use for transient production of saponins in Nicotiana benthamiana. Plant J **84**: 478–490

Khakimov B, Motawia MS, Bak S, Engelsen SB (2013) The use of trimethylsilyl cyanide derivatization for robust and broad-spectrum high-throughput gas chromatography-mass spectrometry based metabolomics. Anal Bioanal Chem **405**: 9193–9205

Khakimov B, Tseng LH, Godejohann M, Bak S, Engelsen SB (2016) Screening for triterpenoid saponins in plants using hyphenated analytical platforms. Molecules **21**: 1–19

Kumar S, Stecher G, Li M, Knyaz C, Tamura K (2018) MEGA X: molecular evolutionary genetics analysis across computing platforms. Mol Biol Evol **35**: 1547–1549

Kuzina V, Ekstrøm CT, Andersen SB, Nielsen JK, Olsen CE, Bak S (2009) Identification of defense compounds in barbarea vulgaris against the herbivore phyllotreta nemorum by an ecometabolomic approach. Plant Physiol **151**: 1977–1990

Kuzina V, Nielsen JK, Augustin JM, Torp AM, Bak S, Andersen SB (2011) Barbarea vulgaris linkage map and quantitative trait loci for saponins, glucosinolates, hairiness and resistance to the herbivore Phyllotreta nemorum. Phytochemistry **72**: 188–198

Leong BJ, Last RL (2017) Promiscuity, impersonation and accommodation: evolution of plant specialized metabolism. Curr Opin Struct Biol **47**: 105–112

Liu Q, Khakimov B, Cárdenas PD, Cozzi F, Olsen CE, Jensen KR, Hauser TP, Bak S (2019) The cytochrome P450 CYP72A552 is key to production of hederagenin-based saponins that mediate plant defense against herbivores. New Phytol **222**: 1599–1609

Lodeiro S, Segura MJR, Stahl M, Schulz-Gasch T, Matsuda SPT (2004) Oxidosqualene cylase second-sphere residues profoundly influence the product profile. ChemBioChem **5**: 1581–1585

Lodeiro S, Xiong Q, Wilson WK, Kolesnikova MD, Onak CS, Matsuda SPT (2007) An oxidosqualene cyclase makes numerous products by diverse mechanisms: a challenge to prevailing concepts of triterpene biosynthesis. J Am Chem Soc **129**: 11213–11222

Lorent JH, Quetin-Leclercq J, Mingeot-Leclercq MP (2014) The amphiphilic nature of saponins and their effects on artificial and biological membranes and potential consequences for red blood and cancer cells. Org Biomol Chem **12**: 8803–8822

Moghe G, Last RL (2015) Something old, something new: conserved enzymes and the evolution of novelty in plant specialized metabolism. Plant Physiol **169**: pp.00994.2015

Moghe GD, Leong BJ, Hurney SM, Jones AD, Last RL (2017) Evolutionary routes to biochemical innovation revealed by integrative analysis of a plant-defense related specialized metabolic pathway. eLife **6**: e28468

Morita M, Shibuya M, Kushiro T, Masuda K, Ebizuka Y (2000) Molecular cloning and functional expression of triterpene synthases from pea (Pisum sativum): new α-amyrin-producing enzyme is a multifunctional triterpene synthase. Eur J Biochem **267**: 3453–3460

Moses T, Papadopoulou KK, Osbourn A (2014) Metabolic and functional diversity of saponins, biosynthetic intermediates and semi-synthetic derivatives. Crit Rev Biochem Mol Biol **49**: 439–462

Moses T, Pollier J, Shen Q, Soetaert S, Reed J, Erffelinck ML, Nieuwerburgh FCWV, Vanden Bossche R, Osbourn A, Thevelein JM, et al. (2015) OSC2 and CYP716A14V2 catalyze the biosynthesis of triterpenoids for the cuticle of aerial organs of Artemisia annua. Plant Cell **27**: 286–301

Nielsen H, Engelbrecht J (1997) Identification of prokaryotic and eukaryotic signal peptides and prediction of their cleavage sites. Protein Eng **10**: 1–6

Nielsen JK, Nagao T, Okabe H, Shinoda T (2010a) Resistance in the plant, Barbarea vulgaris, and counter-adaptations in flea beetles mediated by saponins. J Chem Ecol **36**: 277–285

Nielsen NJ, Nielsen J, Staerk D (2010b) New resistance-correlated saponins from the insect-resistant crucifer barbarea vulgaris. J Agric Food Chem **58**: 5509–5514

Nørholm MHH (2010) A mutant Pfu DNA polymerase designed for advanced uracil-excision DNA engineering. BMC Biotechnol **10**: 21

Papadopoulou K, Melton RE, Leggett M, Daniels MJ, Osbourn AE (1999) Compromised disease resistance in saponin-deficient plants. Proc Natl Acad Sci USA **96**: 12923–12928

Phillips DR, Rasbery JM, Bartel B, Matsuda SP (2006) Biosynthetic diversity in plant triterpene cyclization. Curr Opin Plant Biol **9**: 305–314

Pichersky E, Lewinsohn E (2011) Convergent evolution in plant specialized metabolism. Annu Rev Plant Biol **62**: 549–566

Racolta S, Juhl PB, Sirim D, Pleiss J (2012) The triterpene cyclase protein family: a systematic analysis. Proteins Struct Funct Bioinforma **80**: 2009–2019

Sainsbury F, Thuenemann EC, Lomonossoff GP (2009) PEAQ: versatile expression vectors for easy and quick transient expression of heterologous proteins in plants. Plant Biotechnol J **7**: 682–693

Salmon M, Thimmappa RB, Minto RE, Melton RE, Hughes RK, O'maille PE, Hemmings AM, Osbourn A (2016) A conserved amino acid residue critical for product and substrate specificity in

plant triterpene synthases. Proc Natl Acad Sci USA **113**: E4407–E4414

Segura MJR, Jackson BE, Matsuda SPT (2003) Mutagenesis approaches to deduce structure-function relationships in terpene synthases. Nat Prod Rep **20**: 304–317

Shinoda T, Nagao T, Nakayama M, Serizawa H, Koshioka M, Okabe H, Kawai A (2002) Identification of a triterpenoid saponin from a crucifer, Barbarea vulgaris, as a feeding deterrent to the diamondback moth, Plutella xylostella. J Chem Ecol **28**: 587–599

Shiu SH, Karlowski WM, Pan R, Tzeng YH, Mayer KFX, Li WH (2004) Comparative analysis of the receptor-like kinase family in Arabidopsis and rice. Plant Cell **16**: 1220–1234

Srisawat P, Fukushima EO, Yasumoto S, Robertlee J, Suzuki H, Seki H, Muranaka T (2019) Identification of oxidosqualene cyclases from the medicinal legume tree Bauhinia forficata: a step toward discovering preponderant α-amyrin-producing activity. New Phytol **224**: 352–366

Thimmappa R, Geisler K, Louveau T, O'Maille P, Osbourn A (2014) Triterpene biosynthesis in plants. Annu Rev Plant Biol **65**: 225–257

Thoma R, Schulz-Gasen T, D'Arcy B, Benz J, Aebi J, Dehmlow H, Hennig M, Stihle M, Ruf A (2004) Insight into steroid scaffold formation from the structure of human oxidosqualene cyclase. Nature **432**: 118–122

Wendt KU, Schulz GE, Corey EJ, Liu DR (2000) Enzyme mechanisms for polycyclic triterpene formation. Angew Chemie - Int Ed **39**: 2812–2833

Wu S, Zhang F, Xiong W, Molnár I, Liang J, Ji A, Li Y, Wang C, Wang S, Liu Z, et al. (2020) An unexpected oxidosqualene cyclase active site architecture in the Iris tectorum multifunctional α-amyrin synthase. ACS Catal **10**: 9515–9520

Wu Z, Xu H, Wang M, Zhan R, Chen W, Zhang R, Kuang Z, Zhang F, Wang K, Gu J (2019) Molecular docking and molecular dynamics studies on selective synthesis of α-amyrin and β-amyrin by oxidosqualene cyclases from Ilex Asprella. Int J Mol Sci **20**: 3469

Xu R, Fazio GC, Matsuda SPT (2004) On the origins of triterpenoid skeletal diversity. Phytochemistry **65**: 261–291

Xue Z, Duan L, Liu D, Guo J, Ge S, Dicks J, Ómáille P, Osbourn A, Qi X (2012) Divergent evolution of oxidosqualene cyclases in plants. New Phytol **193**: 1022–1038

Zheng L, Baumann U, Reymond JL (2004) An efficient one-step site-directed and site-saturation mutagenesis protocol. Nucleic Acids Res **32**: e115